

**Atomic steps on the MgO(100) surface**

S. R. Lu, R. Yu,\* and J. Zhu

*Beijing National Center for Electron Microscopy, Key Laboratory of Advanced Materials of Ministry of Education of China and State Key Laboratory of New Ceramics and Fine Processing, School of Materials Science and Engineering, Tsinghua University, Beijing 100084, China*

(Received 27 November 2012; revised manuscript received 15 March 2013; published 24 April 2013)

Defects on insulating surfaces have been studied much less compared to conductors due to experimental difficulties. Here we report quantitative structure analysis of atomic steps on the MgO(100) surface combining aberration-corrected high resolution transmission electron microscopy and density function theory calculations. While the broad faces show little relaxation or rumpling, the atoms at the step sites have significant displacements, depending on the atomic coordination. The general trend is to smooth the steps and lower their formation energy. The angles at the upper and lower corners of the mono-atomic step increase from unrelaxed  $90^\circ$  to  $94^\circ$  and  $101^\circ$ , respectively. The experimentally measured positions of the atoms at the step sites match the density function theory results within several picometers.

DOI: [10.1103/PhysRevB.87.165436](https://doi.org/10.1103/PhysRevB.87.165436)

PACS number(s): 68.47.Gh, 68.37.Og, 68.35.Dv

**I. INTRODUCTION**

MgO is a typical oxide with a rock-salt structure. As a model system of metal oxides, the surface structure of MgO has long been investigated and discussed. Technologically, the MgO surface can be used as a substrate for thin film growth like  $\text{YBa}_2\text{Cu}_3\text{O}_7$ ,<sup>1</sup> as the catalyst of the  $\text{H}_2$  and  $\text{D}_2$  exchange reaction and the dehydrogenation of formic acid or methanol.<sup>2</sup> Steps and terraces on the high-index surface may participate in the chemisorption of  $\text{H}_2$  and water.<sup>3,4</sup> Resolving the structure of surface steps may provide useful information for understanding the active sites for catalysis and the mechanisms of thin film growth.

According to Tasker's classification,<sup>5</sup> the low-index surfaces of MgO can be classified as different types. The {100} and {110} surfaces are typical type I nonpolar surfaces, which involves a sequence of charge-neutral planes. The {111} surface is a type III polar surface, which is a stacking of charged planes of  $\text{Mg}^{2+}$  and  $\text{O}^{2-}$  and the repeat unit taken from the surface has a net dipole. In rock-salt crystal, the surface energy of nonpolar {100} surface is far lower than other surfaces.<sup>6-8</sup> Early low energy electron diffraction (LEED) and helium atom scattering (HAS) studies on cleaved (100) surface of MgO showed that the {100} surface is nearly ideal. The inward relaxation, represented by the distance between the outermost surface layer and the second layer, is no more than 2.5% with respect to the layer distance of {200} planes. And the rumpling is less than 2%.<sup>9</sup> Recently, the fast atom diffraction (FAD) method has been employed to measure the surface rumpling,<sup>10</sup> giving the contraction of the Mg atom towards bulk compared to the O atom is  $(0.03 \pm 0.03) \text{ \AA}$ . The FAD result agreed to their calculations of density function theory (DFT), which gave rumpling of  $0.057 \text{ \AA}$  (2.7% with respect to the layer distance of {200} planes).

The stepped high-index surfaces of MgO were previously identified by TEM and atomic force microscopy (AFM). MgO smoke damaged by abrasion, erode by  $\text{H}_2\text{O}$  vapor and exposed to the vacuum in TEM would cause a surface roughening effect, forming terraces and steps of only a few unit cells, and thus low coordinated ions increased.<sup>11,12</sup> AFM study on the (100) surface showed wide terraces ends with

single and double atomic height steps and other surface defects.<sup>13-16</sup> A defected surface, including terrace and step sites, plays an important role in molecular absorption and reactivity of the MgO surface.<sup>9,17</sup> Relaxation at these sites will change the absorption energy.<sup>18,19</sup> A different theoretical approach, including static lattice computer simulation,<sup>20</sup> Car-Parrinello method,<sup>21</sup> quantum self-consistent method,<sup>22</sup> *ab initio* embedded cluster model,<sup>18</sup> DFT method,<sup>19</sup> and *ab initio* Hartree-Fock method<sup>23</sup> have been used to determine the geometrical structure of surface stepped surfaces. In contrast to many theoretical studies, few experimental works have been done to identify the atomic displacements around the steps quantitatively. The critical requirement in this regard is to measure accurately the atomic positions in a very local area. Although MgO has a simple crystal structure, it is highly insulating, presenting difficulties to conventional surface science techniques like LEED and scanning tunneling microscopy (STM).

In contrast, transmission electron microscopy (TEM) employs high energy electrons as the probe and the charging problem encountered in LEED for insulating materials is mitigated to a large extent. For example, Wang *et al.*<sup>24</sup> used energy-filtering HRTEM imaging to measure an inelastic absorption function of the MgO(100) surface. In the profile imaging mode, where the electron direction is parallel to the surface, the structural information of the outermost surface layer and the layers below it can be obtained simultaneously. The resolution and accuracy of conventional TEM are limited by the aberrations of the objective lens. Recently developed aberration-corrected TEM makes it possible to determine the positions of surface atom quantitatively. Yu *et al.*<sup>25</sup> used aberration-corrected TEM to measure the positions of surface atoms of a cobalt oxide at a subangstrom scale, demonstrating the potential of aberration-corrected TEM in determining the surface structure of oxides.

In this work, the (100) surface of MgO and the steps on it have been investigated as a model system of insulating surfaces. Combining the aberration-corrected TEM experiments and the density-functional theory calculations, atomic relaxation of the surface steps have been analyzed to an accuracy of picometers.

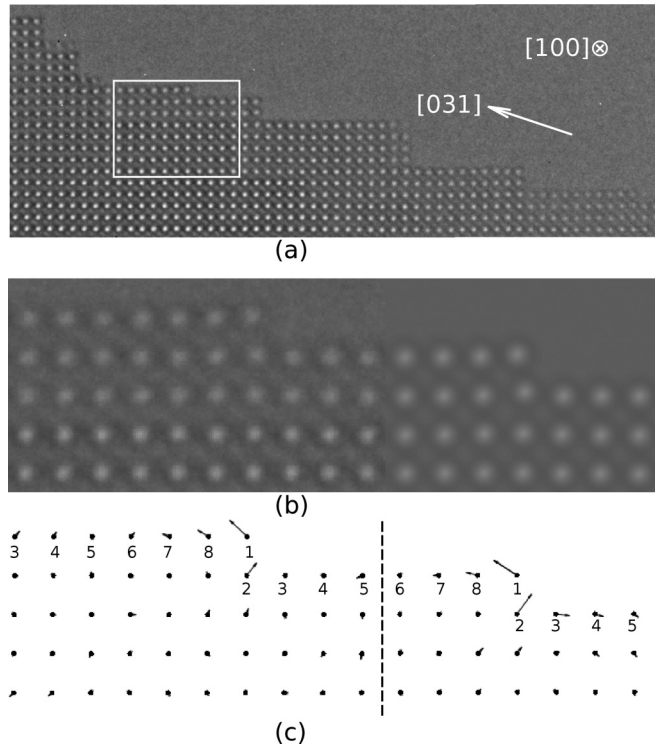


FIG. 1. (a) HRTEM image of MgO high Miller index surface faceted into small  $\{100\}$  surfaces. The atomic columns selected by the white rectangle were used for quantitative measurements. (b) Left: experimental image around the step; right: simulated image using DFT calculation result as input. (c) Visualization of atomic displacements corresponding to the image in (b). All arrows were magnified by 5 times.

## II. EXPERIMENT AND CALCULATION DETAILS

The TEM sample was prepared by mechanically milling MgO single crystal into powder in ethanol, then dispersed by ultrasonic in ethanol, and finally collected on the holey-carbon TEM grid. Ethanol was evaporated under a drying lamp in air. The TEM column where the sample is inserted before observing kept a vacuum of about  $10^{-5}$  Pa.

HRTEM images were taken using the negative-Cs imaging technique<sup>26</sup> in a FEI Titan 80-300 Cs-corrected microscope. The high voltage was 300 keV. The spherical aberration was set to  $-13 \mu\text{m}$  and measured by taking Zemlin tableau<sup>27</sup> of the holey-carbon TEM grid. Other residual aberrations were adjusted and measured to ensure that twofold astigmatism A1 is less than 2 nm. Threefold astigmatism A2 and comma B2 are less than 20 nm. The HRTEM image of the  $[100]$  and  $[110]$  zone axis is obtained, shown in Figs. 1 and 2.

The coordinate of an atomic column was obtained by fitting the image contrast around the column to a 2D Gaussian function using MacTempas<sup>28</sup> software. Using this method, the measurement accuracy of atom position could reach as precise as 5 pm.<sup>29</sup> Extensive image simulations were performed to determine the imaging conditions and to compare with theoretical results. Simulated images were calculated by using the multislice method<sup>30</sup> implemented in the MacTempasX<sup>28</sup> software. Our DFT calculation results were made as the input of HRTEM image simulations. By adjusting imaging parame-

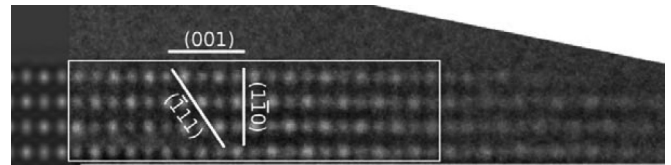


FIG. 2. HRTEM image of MgO in the  $[110]$  zone axis. Left: simulated image, right: experimental image. Atoms in the selected area were used for quantitative measurement of rumpling and layer distance.

ters and comparing simulated images with experimental ones, the experimental imaging conditions were obtained as the parameters for the best correlated image with the maximum likelihood.

The uncertainty in our experiment is derived through a careful checking and calculation. The uncertainties come from several aspects. The image noise contributed most of the random deviations. Standard deviation of Gaussian fitting of a single atom column ranges from 1% to 3% (with respect to the layer distance of  $\{200\}$  planes) in our experimental images. We tested this uncertainty by adding the same amount of noise to the simulated image, and obtained the same deviation. The residual aberrations and sample tilt in the TEM image system also affect the position of the atom column in the image as systematic errors, but it is smaller. We calculated a series of images with different image parameters. Under the worst case in the estimated range of residual aberration and sample tilt in experiment, the uncertainty derived from image aberrations is 1% (with respect to the layer distance of  $\{200\}$  planes). The total uncertainty was estimated by the residual error in fitting the reference lattice and the estimated residual aberration.

The first-principles calculations of the surface steps were done within the density function theory as implemented in the Vienna *ab initio* simulation package (VASP).<sup>31,32</sup> The projector augmented wave method and the Perdew, Burke, and Ernzerhof (PBE)<sup>33,34</sup> exchange-correlation functional were used in the calculations. The energy cutoff and the number of  $k$  points were optimized to ensure the energy convergence to less than 1 meV per surface atom. In the slab model for surface rumpling calculation, we used a super cell with  $a = b = 4.248/\sqrt{2} \text{ \AA}$ ,  $c = 6 \times 4.248 \text{ \AA}$ . Each slab contained seven atomic layers of  $(002)$  planes. The vacuum between two slabs was around  $10 \text{ \AA}$ . The energy cutoff was 550 eV, and a  $11 \times 11 \times 1$  Monkhorst-Pack  $k$ -point mesh was used.

We used the same parameters as in Ref. 35 to characterize the surface rumpling and relaxation, i.e.,  $d_{\text{rum}} = (d_{\text{O}} - d_{\text{Mg}})/d_b$ ,  $d_{\text{rel}} = (d_{\text{O}} + d_{\text{Mg}} - 4d_b)/2d_b$ , where  $d_{\text{O}}$  represents the distance between the O atom in the outermost layer and the third layer,  $d_{\text{Mg}}$  represents the distance between the Mg atom in the outermost layer and the third layer, and  $d_b$  is the  $\{200\}$  layer distance in the bulk. We used the distance between the third and fourth layers as a representation of layer distance in the bulk. This is because in our calculation we found that relaxation and rumpling at the surface only affect the outmost layer and the second layer. The third layer and below relaxes just the same as the bulk.

To calculate the atomic positions around the step, we built a slab model of the  $(107)$  surface which consists of  $(001)$

terraces with a monoatomic step between each terrace. The distance of two neighbor steps along the [100] direction is 7 interatomic distance so far, enough that step-step interactions can be neglected.<sup>36</sup> Each slab contained seven atomic layers and the vacuum between the two slabs was around 10 Å. The energy cutoff and the  $k$ -point density in reciprocal space were kept the same as in the surface rumpling calculations.

### III. RESULTS AND DISCUSSIONS

Low magnification images in the [100] zone axis and the corresponding diffraction patterns (not given here) showed that most profiles are straight and in the {001} orientation, indicating that the {001} surface is most popular, consistent with the fact that the {001} surface has the lowest energy for MgO.

Figure 1 shows a typical HRTEM image of high-index surfaces in the [100] zone axis. In this viewing direction, the (001) and (011) surfaces are edge-on and can be imaged clearly if they exist. In Fig. 1 the surface shown in the lower left is apparently the (013) to (014) surface, but is faceted into small (001) and (010) surfaces at the atomic scale. No periodic reconstruction can be identified on the (001) surface, in agreement with theoretical calculations. The steps have single to several atoms in height. There is no change in contrast from the broad faces to the steps, indicating that the steps are in the [100] direction.

The formation of the low-energy facets on high-index surfaces may be attributed to the exposure to the H<sub>2</sub>O vapor in air during the sample preparation and the electron irradiation during TEM observations. It has been reported that MgO particles can be eroded by the exposure to H<sub>2</sub>O vapor and the electron irradiation in TEM.<sup>11,37</sup> As atoms are removed slowly from the particles in those processes, the thermodynamically low-energy facets are produced. In our TEM observations, the electron beam was employed to generate clean surfaces *in situ* inside TEM. The surface atoms were removed gradually layer by layer by electron beam, ensuring that the surface of the observed area was always clean and fresh without contaminations.

From the [100] viewing direction, we measured the atomic displacements around the steps. We quantitatively measured the positions of atomic columns in the selected rectangular area in Fig. 1(a) by 2D Gaussian fitting. To calculate the exact displacements of surface atoms we built an ideal reference lattice of bulk MgO, based on fitting the atom positions of the bulk MgO to an ideal 2D lattice by the least-square method. We also used image simulations to compare the experimental result with DFT calculations. The arrows in Fig. 1(c) show the atom displacements in the simulated and experimental TEM images. All arrows were magnified by 5 times.

The atoms at steps have lower coordination numbers than those inside the bulk or at broad surfaces. The low-coordinate atomic columns are labeled in Fig. 1(c). Atoms at position 1, 2, 3, and 8 have a coordination number of 4, 6, 5, and 5, respectively. In the [100] viewing direction, the Mg and O atoms are overlapping and indistinguishable in TEM images. Therefore, the measured atomic positions were the average of the Mg and O atoms. Based on the measured positions in the experimental images, the “bond lengths” and “bond angles” of

TABLE I. Bond lengths and bond angles in experimental and simulated images, which are based on the DFT calculations.

Parameter	Experimental image	Simulated image
Bond 8-1	2.03 Å ± 0.10 Å	1.99 Å
Bond 1-2	2.17 Å ± 0.10 Å	2.10 Å
Bond 2-3	2.02 Å ± 0.10 Å	2.11 Å
Angle 8-1-2	94.4° ± 3.5°	96.1°
Angle 1-2-3	100.8° ± 3.5°	103.6°

the low-coordinate atomic columns were calculated and listed in Table I, together with those derived from the simulated images of DFT relaxations.

The error bar was calculated by adding the random error (estimated by the residual error in fitting the reference bulk lattice) to the systematic error (estimated by image simulation). The random errors of bond length and bond angle under 95% confidence level were 0.08 Å and 2.5°, respectively. The systematic errors of bond length and bond angle were no more than 0.02 Å and 1.0°, respectively. So the final error bars of bond length and bond angle were 0.10 Å and 3.5°.

Table II listed bond lengths and bond angles in the DFT calculations. Because the lattice parameter used in the DFT calculation is slightly different from the experimental one,  $a_{\text{expt}}/a_{\text{DFT}} = 0.9925$ , all lengths derived from DFT calculations were multiplied by this scale factor to match the experimental result.

The experimental results are consistent with the DFT calculations within the uncertainties. In both experimental and calculation results, the largest displacements occur at the upper and lower edges of the step [positions 1 and 2 in Fig. 1(c)]. The general trend of relaxation is to “smooth” the surface steps. Calculated bond lengths between positions 1 and 8, and that between 1 and 2, are smaller than the relaxed flat (001) surface. On the relaxed flat (001) surface the calculated bond length between the Mg atom in the outmost layer and the O atom in the second layer is 2.09 Å, and bond length between the O atom in the outmost layer and the Mg atom in the second layer is 2.13 Å. Besides, bond angles connecting the low-coordinate atoms are larger than 90°. Previous calculations of stepped surfaces by Tasker,<sup>20</sup>

TABLE II. Bond lengths and bond angles in DFT calculations.

Parameter	DFT relaxed structure
Bond Mg8-O1	2.02 Å
Bond O8-Mg1	1.97 Å
Bond Mg1-O2	2.06 Å
Bond O1-Mg2	2.09 Å
Bond Mg2-O3	2.09 Å
Bond O2-Mg3	2.13 Å
Angle Mg8-O1-Mg2	95.5°
Angle O8-Mg1-O2	100.1°
Angle Mg1-O2-Mg3	108.2°
Angle O1-Mg2-O3	106.3°
Angle Mg1-O1-Mg1	174.5°
Angle Mg2-O2-Mg2	177.6°

TABLE III. In-plane and out-of-plane rumpling at surface step of MgO.

Position	1	2	3	4	5	6	7	8
Out-of-plane rumpling/Å	0.071	-0.037	0.056	0.049	0.050	0.050	0.053	0.040
In-plane rumpling/Å	0.072	-0.023	-0.014	0.004	0.000	-0.001	0.006	-0.025

Goniakowski,<sup>22</sup> and Kantorovich<sup>19</sup> are qualitatively consistent with present experimental and calculation results.

Besides the rumpling normal to the (100) surface, rumpling at the step edges has a component within the surface plane. Similar to the definition of the “out-of-plane” rumpling on the broad (001) plane, we define “in-plane” rumpling positive for that with cations moving into the bulk (in our case is [010] direction) while the anions moving towards the vacuum ([0 $\bar{1}$ 0] direction). That is to say, the out-of-plane rumpling is defined as  $(z_O - z_{Mg})/d_b$ , and the in-plane rumpling is defined as  $(y_{Mg} - y_O)/d_b$ , where  $y_O$ ,  $z_O$ ,  $y_{Mg}$ ,  $z_{Mg}$  are the coordinates of the O and Mg atoms,  $d_b$  is the {200} layer distance in the bulk. Here we use the reference lattice parameter for  $d_b$ . Atoms at the upper edge [position 1 in Fig. 1(c)] have positive in-plane rumpling of 0.072 Å. This in-plane positive rumpling at position 1 influences atoms at the lower edge [position 2 in Fig. 1(c)], which show very small negative rumpling. Both an out-of-plane rumpling and in-plane rumpling value is listed in Table III. In order to directly compare these values with the rumpling of the flat (001) surface, we also measured and calculated the rumpling of the flat (001) surface.

Figure 2 shows the (001) surface viewed in the [110] direction. The advantage of viewing the (001) surface in the [110] direction is that the Mg and O atomic columns were separately imaged in the direction, making it ideal for measuring the surface rumpling quantitatively. Although the ( $\bar{1}$ 11) and ( $\bar{1}$ 10) surfaces should also be viewed edge-on in the direction, they were never observed in our experiments. This is consistent with the fact that the {001} surface has a far lower energy than the ( $\bar{1}$ 10) and ( $\bar{1}$ 11) surfaces. In fact, the ( $\bar{1}$ 10) surface has been faceted into small {001} faces, as revealed by the image contrast. The brightness of the atomic columns decreases from the center to the right edge in the [1 $\bar{1}$ 0] direction, indicating that the sample thickness decreases in that direction.

Also by 2D Gaussian fitting and least-square fitting we acquired the ideal reference lattice. And from the reference lattice we had the basic vectors normal to and parallel to the (001) surface. By projecting the atomic coordinates to the surface normal, the rumpling and relaxation of the outermost layers were determined. We measured the atomic coordinates inside the selected rectangle area shown in Fig. 2 to determine the rumpling and relaxation of the outermost surface layer. The results were  $d_{rum} = 1\% \pm 3\%$  and  $d_{rel} = 3\% \pm 4\%$  (with respect to the layer distance of {200} planes). The uncertainty was also estimated by adding the systematic error 2 pm (1% with respect to the layer distance of {200} planes) to the random error of 95% confidence level. Although the signal to noise ratio in Fig. 2 was worse than Fig. 1, the random error (2% and 3% for  $d_{rum}$  and  $d_{rel}$ ) was smaller here than of the bond length in Fig. 1. Because to calculate the rumpling and relaxation of a layer, the average position in a layer was calculated, so the random error decreased by  $1/\sqrt{n}$  with the number of one kind

of ions  $n$ . Our experimental results showed that the surface rumpling and relax, if they exist, should be quite small.

The DFT calculations gave the relative surface rumpling and relaxation values of 2.36% (0.050 Å) and 0.12% (0.003 Å), respectively. The data are very close to Schüller’s recent DFT calculations.<sup>10</sup> The current experimental result of  $d_{rum}$  by direct imaging are also close to recent experimental results by GIXS (grazing incidence x-ray scattering)<sup>38</sup> and FAD.<sup>10</sup> Although the experimental result of  $d_{rel}$  slightly differs from them, they are within the uncertainties. In literature the surface rumpling and relaxation had long been discussed. Recently the primary reason for the surface rumpling of alkaline-earth metal oxides is thought not to be the ratio of polarizabilities of cations and anions, but the electrostatic energy and valence repulsion effects.<sup>35,39</sup> This helps to explain the positive rumpling of MgO, and negative rumpling of other alkaline-earth metal oxides.

We use a DFT calculation to further analyze how the rumpling and relaxation at surface and step affected the total energy. Surface energy is given as  $\sigma = (E_1 - E_0)/A$ , where  $E_1$  is the energy of the surface supercell and  $E_0$  is the energy of the bulk supercell of the same number of atoms.  $A$  is the surface area in the unit cell. An ideal (001) surface without relaxation and rumpling has a surface energy of  $\sigma_{ideal} = 58.48 \text{ meV}/\text{Å}^2$  (0.936 J/m<sup>2</sup>). After fully structural relaxation, the surface energy decreased to  $\sigma_{relaxed} = 57.18 \text{ meV}/\text{Å}^2$  (0.916 J/m<sup>2</sup>). Our result of surface energy and relaxation energy is very close to previous DFT calculations also using GGA approximation.<sup>35</sup> The energy of surface rumpling and relaxation is  $\Delta\sigma = -1.30 \text{ meV}/\text{Å}^2$  or 0.021 J/m<sup>2</sup>. Therefore, the rumpling has a small stabilizing effect for the (001) surface of MgO. We can separate the energy term into two parts,  $\Delta\sigma = \Delta\sigma_{rel} + \Delta\sigma_{rum}$ , each corresponding to the structure relaxation and rumpling. The energy of an intermediate structure is calculated, where we make the position of every layer of the Mg atom and the O atom artificially fixed to their average position along the [001] direction.  $\Delta\sigma_{rel}$  is the energy difference between the unrelaxed structure and the intermediate structure, and  $\Delta\sigma_{rum}$  is the energy difference between the intermediate structure and the fully relaxed structure. On the flat (001) surface of MgO,  $\Delta\sigma_{rel}$ , i.e., a relaxation without rumpling, changes the surface energy very little ( $|\Delta\sigma_{rel}| < 0.01 \text{ meV}/\text{Å}^2$  or  $< 10^{-4} \text{ J/m}^2$ ).

Tasker<sup>20</sup> suggested that the stepped surface energy can be written as  $E_s = E_{001} \cos \theta + E_{step} \frac{\sin \theta}{\alpha} + E_{int} \frac{\sin \theta}{\alpha}$ . Where  $E_{001}$  is the surface energy of the (001) surface,  $E_{step}$  is the step energy, and  $E_{int}$  is the remaining step-step interaction term. In our (107) surface  $E_{int}$  is sufficiently small and can be neglected. So the step energy can be simply written as  $E_{step} = \gamma = (E_2 - E_1)/l$ , where  $E_2$  is the energy of the supercell containing a pair of steps (we have one step in each side of the slab).  $E_1$  is the energy of the surface supercell which has the

same number of atoms.  $l$  is the total length of the two steps in the supercell. We calculated that from the relaxed surface unit cell to the relaxed stepped unit cell the formation energy  $\gamma_{\text{relaxed}} = -188 \text{ meV}/\text{\AA}$  or  $-3.01 \times 10^{-10} \text{ J/m}$ . Our value of  $\gamma_{\text{relaxed}}$  lies between previous results using the static lattice method ( $-3.72 \times 10^{-10} \text{ J/m}$ )<sup>20</sup> and quantum self-consistent method ( $-2.7 \times 10^{-10} \text{ J/m}$ ).<sup>22</sup> Our result is closer to the latter, although our relaxed structure model is closer to the former. We also calculated that from the unrelaxed surface unit cell to the unrelaxed stepped unit cell, the formation energy  $\gamma_{\text{unrelaxed}} = -305 \text{ meV}/\text{\AA}$  ( $-4.89 \times 10^{-10} \text{ J/m}$ ). Relaxation energy at step site is  $\Delta\gamma = \gamma_{\text{unrelaxed}} - \gamma_{\text{relaxed}} = -118 \text{ meV}/\text{\AA}$  ( $-1.88 \times 10^{-10} \text{ J/m}$ ).  $\Delta\gamma$  is about 38% of  $\gamma_{\text{unrelaxed}}$ . So we could see the relaxation at the step significantly lowered the formation energy of steps.

#### IV. CONCLUSION

We have investigated the structure of steps at the MgO(100) surface combining aberration-corrected TEM with first-

principles calculations. Subangstrom measurements show that the relaxation is negligibly small on the broad (100) surface. Atomic displacements around the steps, however, are significant. The general trend is to smooth the steps, with the bond angle at the upper edge enlarged from  $90^\circ$  to  $94^\circ$ , and that at the lower edge enlarged to  $101^\circ$ . Compared to the ideal step, the relaxation at the step lowers significantly (38%) the step energy.

#### ACKNOWLEDGMENTS

This work was supported by NSFC (51071092), National Basic Research Program of China (2011CB606406, 2009CB623701), the Foundation for the Author of National Excellent Doctoral Dissertation of China, Program for New Century Excellent Talents in University, and the project sponsored by SRF for ROCS, SEM. This work made use of the resources of the Beijing National Center for Electron Microscopy and Shanghai Supercomputer Center.

\*ryu@tsinghua.edu.cn

<sup>1</sup>B. H. Moeckly, S. E. Russek, D. K. Lathrop, R. A. Buhrman, J. Li, and J. W. Mayer, *Appl. Phys. Lett.* **57**, 1687 (1990).

<sup>2</sup>M.-C. Wu, C. A. Estrada, J. S. Corneille, and D. W. Goodman, *J. Chem. Phys.* **96**, 3892 (1992).

<sup>3</sup>H. Onishi, C. Egawa, T. Aruga, and Y. Iwasawa, *Surf. Sci.* **191**, 479 (1987).

<sup>4</sup>N. H. de Leeuw, G. W. Watson, and S. C. Parker, *J. Phys. Chem.* **99**, 17219 (1995).

<sup>5</sup>P. W. Tasker, *J. Phys. C* **12**, 4977 (1979).

<sup>6</sup>P. W. Tasker, *Adv. Ceram.* **10**, 176 (1984).

<sup>7</sup>W. C. Mackrodt and P. W. Tasker, *Chem. Br.* **21**, 366 (1985).

<sup>8</sup>A. Gibson, R. Haydock, and J. P. LaFemina, *J. Vac. Sci. Technol. A* **10**, 2361 (1992).

<sup>9</sup>V. E. Henrich and P. A. Cox, *The Surface Science of Metal Oxides* (Cambridge University Press, Cambridge, 1996).

<sup>10</sup>A. Schüller, D. Blauth, J. Seifert, M. Busch, H. Winter, K. Gärtner, R. Włodarczyk, J. Sauer, and M. Sierka, *Surf. Sci.* **606**, 161 (2012).

<sup>11</sup>C. F. Jones, R. A. Reeve, R. Rigg, R. L. Segall, R. S. C. Smart, and P. S. Turner, *J. Chem. Soc., Faraday Trans. 1* **80**, 2609 (1984).

<sup>12</sup>S. Coluccia, A. J. Tench, and R. L. Segall, *J. Chem. Soc., Faraday Trans. 1* **75**, 1769 (1979).

<sup>13</sup>C. Barth and C. Henry, *Phys. Rev. Lett.* **91**, 196102 (2003).

<sup>14</sup>D. Abriou, F. Creuzet, and J. Jupille, *Surf. Sci.* **352–354**, 499 (1996).

<sup>15</sup>T. V. Ashworth, C. L. Pang, P. L. Wincott, D. J. Vaughan, and G. Thornton, *Appl. Surf. Sci.* **210**, 2 (2003).

<sup>16</sup>K.-i. Fukui and Y. Iwasawa, *Surf. Sci.* **441**, 529 (1999).

<sup>17</sup>M. Boudart, A. Delbouille, E. G. Derouane, V. Indovina, and A. B. Walters, *J. Am. Chem. Soc.* **94**, 6622 (1972).

<sup>18</sup>E. V. Stefanovich and T. N. Truong, *J. Chem. Phys.* **102**, 5071 (1995).

<sup>19</sup>L. N. Kantorovich, J. M. Holender, and M. J. Gillan, *Surf. Sci.* **343**, 221 (1995).

<sup>20</sup>P. W. Tasker and D. M. Duffy, *Surf. Sci.* **137**, 91 (1984).

<sup>21</sup>W. Langel and M. Parrinello, *Phys. Rev. Lett.* **73**, 504 (1994).

<sup>22</sup>J. Goniakowski and C. Noguera, *Surf. Sci.* **340**, 191 (1995).

<sup>23</sup>A. L. Shluger, P. V. Sushko, and L. N. Kantorovich, *Phys. Rev. B* **59**, 2417 (1999).

<sup>24</sup>Z. L. Wang and A. J. Shapiro, *Ultramicroscopy* **60**, 115 (1995).

<sup>25</sup>R. Yu, L. H. Hu, Z. Y. Cheng, Y. D. Li, H. Q. Ye, and J. Zhu, *Phys. Rev. Lett.* **105**, 226101 (2010).

<sup>26</sup>C. L. Jia, M. Lentzen, and K. Urban, *Science* **299**, 870 (2003).

<sup>27</sup>F. Zemlin, K. Weiss, P. Schiske, W. Kunath, and K.-H. Herrmann, *Ultramicroscopy* **3**, 49 (1978).

<sup>28</sup>R. Kilaas, in *Proceedings of the 45th Annual Meeting of the Electron Microscopy Society of America, Baltimore, MD*, edited by G. W. Bailey (1987), p. 66.

<sup>29</sup>C.-L. Jia, S.-B. Mi, K. Urban, I. Vrejoiu, M. Alexe, and D. Hesse, *Nat. Mater.* **7**, 4143 (2008).

<sup>30</sup>J. M. Cowley, *Diffraction Physics* (Elsevier Science B.V., New York, 1995).

<sup>31</sup>G. Kresse and J. Furthmüller, *Phys. Rev. B* **54**, 11169 (1996).

<sup>32</sup>G. Kresse and J. Furthmüller, *Comput. Mater. Sci.* **6**, 15 (1996).

<sup>33</sup>J. P. Perdew, K. Burke, and M. Ernzerhof, *Phys. Rev. Lett.* **77**, 3865 (1996).

<sup>34</sup>J. P. Perdew, K. Burke, and M. Ernzerhof, *Phys. Rev. Lett.* **78**, 1396 (1997).

<sup>35</sup>N. V. Skorodumova, K. Hermansson, and B. Johansson, *Phys. Rev. B* **72**, 125414 (2005).

<sup>36</sup>P. W. Tasker, *Adv. Ceram.* **10**, 176 (1984).

<sup>37</sup>C. F. Jones, R. L. Segall, R. S. C. Smart, and P. S. Turner, *Radiat. Eff.* **60**, 167 (1982).

<sup>38</sup>O. Robach, G. Renaud, and A. Barbier, *Surf. Sci.* **401**, 227 (1998).

<sup>39</sup>D. R. Alfonso, J. A. Snyder, J. E. Jaffe, A. C. Hess, and M. Gutowski, *Phys. Rev. B* **62**, 8318 (2000).